Mitotic catastrophe cell death induced by heat shock protein 90 inhibitor in BRCA1-deficient breast cancer cell lines

Magdalena Zajac,[1] Maria Victoria Moneo,[2] Amancio Carnero,[2] Javier Benitez,[1,3] and Beatriz Martínez-Delgado[1,3]

[1]Human Genetics Group and [2]Assay Development Group, Spanish National Cancer Centre, Madrid, Spain and [3]Centre for Biomedical Networking Research on Rare Diseases, Madrid, Spain

Abstract

Heat shock protein 90 (Hsp90) is a molecular chaperone involved in folding, assembly, maturation, and stabilization of the client proteins that regulate survival of malignant cells. As previous reports correlate high Hsp90 expression with decreased survival in breast cancer, Hsp90 may be a favorable target for investigational therapy in breast cancer. In our study, we have examined the response of a panel of both BRCA1-null (UACC 3199, HCC 1937, and MBA-MD-436) and BRCA1-wt breast cancer cell lines (MCF-7, MBA-MD-157, and Hs578T) to determine the proteins governing response to Hsp90 inhibitor 17-allyloamino-17-demethoxy-geldanamycin. On treatment with the drug, cells arrested at G_2-M phase and entered aberrant mitosis in a BRCA1-dependent manner. Failure to arrest the cells at or before mitosis resulted in formation of micronucleated cells, aberrant segregation of chromosomes, microtubule misalignment, and multicentrosomes, leading in eventual mitotic catastrophe cell death. Our observations show that BRCA1 mediates G_2-M transition mainly through chek1 on 17-allyloamino-17-demethoxy-geldanamycin treatment. [Mol Cancer Ther 2008;7(8):2358–66]

Introduction

The heat shock protein 90 (Hsp90) inhibitor, 17-allyloamino-17-demethoxy-geldanamycin (17-AAG), a geldanamycin analogue, is currently in phase II clinical trials[4] (1), in several cancers (2–5), as one of so-called pleiotropic effect drugs, affecting numerous cellular signaling pathways simultaneously. Hsp90 is a chaperone for several oncogenic client proteins (Erbb2, c-Raf, Cdk4, Akt, steroid hormone receptors, mutant p53, hypoxia-inducible factor-1α, survivin, and telomerase hTERT) involved in transcriptional regulation, signal transduction, and cell cycle control as well as in other crucial steps leading to malignant phenotype, invasion, angiogenesis, and metastasis (6, 7). Hsp90 inhibition leads to proteosomal degradation of its client proteins. In cancer cells, Hsp90 is reported to have a constitutive expression and most importantly 100-fold higher binding affinity for 17-AAG than does Hsp90 from normal cells (1). The downstream effects of the Hsp90 inhibition are very complex and depend on the biochemical features and molecular background of the cell type. The reported cell cycle effects are predominantly G_1 (8, 9) and G_2-M block (3, 4, 10). The G_2-M arrest has been observed independently of p53 and Rb status, yet several key regulatory proteins of G_2-M transition (Chek1, Cdk1, Wee1, Myt1, and Polo-1 kinase) have been identified as Hsp90 client proteins,[5] degradation of which may explain the substantial G_2-M peak in cell cycle on treatment. When damage to the mitotic apparatus is excessive, the G_2-M checkpoint will finally adapt. Failure to arrest the cells at or before mitosis results in formation of micronucleated cells, aberrant segregation of chromosomes, microtubule misalignment, multicentrosomes, multipolar mitoses, and aneuploidy, leading to eventual cell death (11). Mitotic catastrophe is a term used to describe these failures in mitosis, reported previously in literature (3, 12–15). Accumulating evidence has implicated Brca1 as a key regulator of the DNA damage checkpoint response, the S and G_2-M checkpoint (16). Studies by Yarden et al. (17) show that Brca1 is necessary to activate chek1-induced DNA damage G_2-M arrest. On top of that, neat investigation by Bae et al. (18) show that Brca1 knockdown cells cause down-regulation in expression of several cell cycle regulatory proteins taking part in mitosis/anaphase progression, cytokinesis, centrosome function, chromosome progression, and spindle checkpoint.

In our work, we have examined the response of a panel of breast cancer cell lines to Hsp90 inhibitor, 17-AAG. We found that this drug induces mitotic catastrophe more significantly in hereditary breast cancer cell lines and showed that Brca1 mediates this response probably through the regulation of chek1 protein.

Received 4/4/08; revised 5/27/08; accepted 5/30/08.

Grant support: Ministerio de Education y Ciencia, SAF06-06140 and Asociación Española Contra el Cáncer.

The costs of publication of this article were defrayed in part by the payment of page charges. This article must therefore be hereby marked *advertisement* in accordance with 18 U.S.C. Section 1734 solely to indicate this fact.

Requests for reprints: Beatriz Martínez-Delgado, Grupo Genética Humana, Centro Nacional de Investigaciones Oncológicas, Melchor Fernández Almagro 3, 28029 Madrid, Spain. Phone: 34-91-224-69-50; Fax: 34-91-224-69-23. E-mail: bmartinez@cnio.es

doi:10.1158/1535-7163.MCT-08-0327

[4] See http://www.clinicals.gov.

[5] Summarized on the Picard laboratory homepage: http://www.picard.ch/DP/DPhome.html.

Materials and Methods

Breast Cancer Cell Lines

Six breast cancer cell lines were included in this study. Three of them corresponded to sporadic breast cancer tumors (MCF-7, MBA-MD-157, and Hs578T), which are BRCA1-wt. The other three corresponded to BRCA1-null cell lines: two of them derived from hereditary Brca1 mutated breast tumors (HCC 1937 and MBA-MD-436) and another one (UACC 3199) presents somatic inactivation of BRCA1. Breast cancer cell lines, MCF-7, UACC 3199, and Hs578T, were obtained from Cancer Epigenetic Group at Spanish National Cancer Centre. HCC 1937 and MBA-MD-157 was kindly provided by Dr. P. Edwards (Department of Pathology, University of Cambridge) and MBA-MD-436 was provided by Dr. K.S Massey-Brown (Department of Pharmacology and Toxicology, University of Arizona). Biological and molecular characteristics of the breast cancer cell lines are presented in Table 1. Normal breast tissue was obtained from breast reduction surgery of healthy women.

Drugs

17-AAG (Sigma-Aldrich) was prepared as a 1 mmol/L stock in DMSO and stored at −20°C and freshly dissolved immediately before use.

Cytotoxicity Assay

To evaluate the antiproliferative effects of inhibitor Hsp90, cells were incubated for 96 h with serial dilutions of the drug from initial 50 μmol/L. Each concentration was assayed in triplicate and then incubated with MTT substrate. The resulting absorbance was measured by means of a microplate reader (Bio-Rad), and the cytotoxic effect of each treatment was assessed by IC_{50} value (concentration of the drug leading to 50% cell survival).

Cell Cycle and Apoptosis Analysis

Cells were seeded in 10 cm dishes at a moderate density in 20 mL complete medium. At 24 h after plating, cells were treated with 500 nmol/L 17-AAG or DMSO (0.1%) as a control. At appropriate intervals (24 and 48 h on treatment with the drug), cells were harvested, fixed with 70% methanol, and washed twice with PBS. After incubation in PBS supplemented with RNase (10 mg/mL; Qiagen) and propidium iodide (PI; 5 mg/mL; Sigma-Aldrich) for 30 min the DNA content was analyzed by FACScan flow cytometer (Becton Dickinson) and CellQuest software.

For apoptosis analysis, cells were harvested and analyzed by flow cytometry using simultaneous staining with Annexin V/APC (BD PharMingen) and PI.

Mitotic Index

The cells on treatment with 500 nmol/L 17-AAG or DMSO (0.1%) for 48 h were harvested and costained according to the manufacturer's instructions with phospho-histone H3 (Ser^{10}) antibody, Alexa Fluor 488–conjugated antibody (Cell Signaling Technology), and PI. In this assay, the fraction of cells that incorporates PI and costains with anti-phospho-histone H3 antibody is considered as to be at the onset of mitosis. The percentage of mitotic cells was determined by fluorescence-activated cell sorting analysis.

Western Blot Analysis

Western blot analysis was done using standard procedures for whole-cell extracts from cell lines. Lysates were prepared using radioimmunoprecipitation assay buffer (Sigma-Aldrich). Equal amounts of protein lysates (50-100 μg) were separated by SDS-PAGE on 10% gels and electrotransferred to Immobilon-P membranes (Millipore) and probed with indicated primary antibody. Antibodies used include Cdc25C (Abcam), phospho-Cdc2 (Tyr^{15}; Cell

Table 1. Molecular and biochemical features of breast cancer cell lines used in the study

	MCF-7	MBA-MD-157	Hs578T	MBA-MD-436	HCC 1937	UACC 3199 (*)
Tumor type*	Human breast adenocarcinoma	Medullary carcinoma	Invasive ductal carcinoma	Human breast adenocarcinoma	Human breast carcinoma	Ductal carcinoma
Molecular subtypes†	Luminal	Mesenchymal	Mesenchymal	Basal	Basal	
TP53 status‡	Wild-type	Mutant	Mutant	Mutant	Mutant	
ER‡	+	−	−	−	−	−
Brca1 (allelic lost/ mutation status)§	Loss/wt	Loss/ wt	Loss/wt	Loss/mutated	Loss/mutated	Loss/methylated
Effects after 17-AAG treatment						
IC_{50} (μmol/L)	0.032 ± 0.0092	0.00148	0.057 ± 0.021	0.059 ± 0.017	0.014 ± 0.006	0.013 ± 0.006
Cell cycle effect	G_2-M arrest	G_2-M arrest	G_2-M arrest	G_2-M arrest	G_2-M arrest	G_2-M arrest
SA-β-galactosidase staining	None	None	None	None	None	None
Mitotic entrance	Low	None	Low	High	High	High
Predominant cell death	Apoptosis	Apoptosis	Apoptosis	Mitotic catastrophe	Mitotic catastrophe	Mitotic catastrophe

*Data derived from the American Type Culture Collection.
†From ref. 29.
‡From ref. 30.
§From ref. 31.

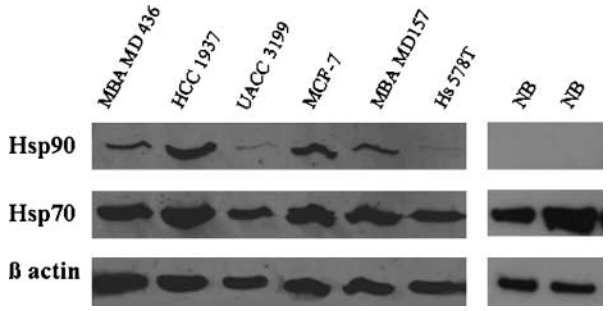

Figure 1. Overexpression of Hsp90 in a panel of hereditary and sporadic cell lines. No expression of Hsp90 detected in normal breast tissue samples (*NB*). Hsp70 was equally highly expressed in both normal samples and tumor cells. Levels of protein were evaluated by Western blot.

Signaling), cyclin B1 (Santa Cruz Biotechnology), phospho-Cdc25C (Ser^{216}; Cell Signaling), Akt (Cell Signaling), Chek1 (Santa Cruz Biotechnology), Cdc2 p34 (Santa Cruz Biotechnology), Aurora B (Abcam), Plk1 (Abcam), survivin (R&D Systems), Hsp90 (Novocastra), Hsp70 (Santa Cruz Biotechnology), and β-actin (Sigma-Aldrich). Alexa Fluor 680–labeled secondary antibodies (1:3,000 dilution; Invitrogen) were used subsequently and Odyssey Infrared detection system (LI-COR Biosciences) applied to visualize blots.

Live Cell Imaging

A fluorescence microscope (Leica AF6000; Leica Systems) equipped with CCD camera was used for live cell imaging. Briefly, 1×10^6 cells were seeded at six-well plates in 1 mL culture medium, and after 24 h after plating, 17-AAG or DMSO was added to a final concentration of 500 nmol/L or 0.1%, respectively. The plate was placed onto a prewarmed microscope stage. The samples were maintained at 37°C and 5% CO_2. Changes in cell morphology were observed for up to 72 h. Images were captures at a rate 1 frame every 10 min using Leica Application Suite advanced fluorescence software 1.5.1 (Leica Systems). Movie files were generated with QuickTime software.

Confocal Microscopy Analysis

Cells were grown for 48 h on coverslips at a moderate confluency with 500 nmol/L 17-AAG. After this time, cells were fixed in cold methanol (−20°C, 5 min). Blocking was done in 5% bovine serum albumin-PBS for 30 min at 37°C followed by incubation with α-tubulin (Sigma-Aldrich) for 1 h at 37°C. Alexa Fluor 488 anti-mouse secondary antibody (Molecular Probes) was applied subsequently.

Nuclear morphology was visible with 4,6′-diaminidino-2-phenylindole (Molecular Probes). Images were processed with the Leica Confocal software.

Small Interfering RNA and Transfection

The Brca1 small interfering RNA (siRNA) were designed and synthesized by Ambion. Three siRNA duplexes recognizing different sequences were tested. Chek1 siRNA sequence was described previously (19). We used a scramble siRNA (Qiagen) as a control. Transfection was carried out using Oligofectamine (Invitrogen) following the manufacturer's instructions and analyzed 24, 36, 48, and 72 h post-transfection. Brca1 and Chek1 mRNA levels were examined. For the experiment with 17-AAG, we have chosen the siRNA decreasing the mRNA levels to 50% of control levels.

Quantitative Reverse Transcription-PCR Analysis

Total RNA (1 μg) was reverse transcribed using MMLV reverse transcriptase (Invitrogen) and random primers. The cDNAs were subjected to quantitative real-time PCR assay with the use of labeled probes for Brca1 and Chek1 (Roche Universal Probe Library) and the TaqMan Universal PCR Mix in an ABI Prism 7900 System (Applied Biosystems) under the manufacturer's recommendations. The PCR amplification was carried out with 10 min at 95°C, followed by 50 cycles of 15 s at 95°C and 1 min at 60°C, using the oligonucleotides shown in Supplementary Table S1.[6] β-Actin was used as internal control and allowed normalization of the samples. All experiments were analyzed in triplicate.

Statistical Analysis

Student's *t* test was used to estimate differences in the mitotic indexes between sporadic and hereditary cell lines.

Results

Overexpression of Hsp90 Protein in Breast Cancer Cell Lines

Initially, we evaluated the expression of Hsp90 in a panel of six breast cancer cell lines and compared the protein expression levels with normal breast tissue. Western blot analysis has displayed Hsp90 expression in the entire set of cell lines examined (Fig. 1). Although the level of Hsp90 expression varied among the different cell lines, these variations were not associated with the Brca1 status of the cells. As for normal breast tissue samples, no positive staining for Hsp90 was detected. Hsp70 was equally highly expressed in both normal samples and tumorigenic cells.

17-AAG Inhibited Cell Growth of Breast Cancer Cell Lines

We have analyzed the effect of 17-AAG on breast cancer cell growth. Sensitivity to 17-AAG was assessed by MTT test and showed both cytotoxic and cytostatic effects. The Hsp90 inhibitor showed cell growth inhibition in a dose-dependent manner for 96 h after treatment. The IC_{50} values are represented in Table 1. The results indicate that sensitivity to the drug was not related to the level of Hsp90 expression of a particular cell line. No significant difference in the sensitivity to 17-AAG was found between BRCA1-wt and BRCA1-null cell lines. IC_{50} values varied between 0.014 ± 0.006 and 0.059 ± 0.017 μmol/L (Table 1). It is known that Hsp90 in normal cells exists in an uncomplexed form that has low affinity for Hsp90 inhibitor. Taking that into account, we have done series of experiments on normal lymphocytes. As expected, the cytotoxicity tests showed weaker effect of the drug on

[6] Supplementary material for this article is available at Molecular Cancer Therapeutics Online (http://mct.aacrjournals.org/).

normal lymphocytes compared with tumor cells, with an IC_{50} value ~30-fold higher (1.96 μmol/L). Moreover, it has been described previously that normal mammary epithelial cells (HMEC) are less sensitive to Hsp90 inhibition than tumor cells with IC_{50} values of 0.943 ± 0.290 μmol/L. Similar results were obtained when analyzing normal and malignant human breast tissue samples; the IC_{50} was reported to be 6.17 ± 1.06 for normal breast versus 0.029 ± 0.004 μmol/L for breast carcinomas (1). Importantly, breast tumors are more sensitive to Hsp90 inhibitor than normal cells.

17-AAG Arrested Cells in G_2-M

We have further explored the effect of 17-AAG on cell cycle arrest (Fig. 2). Control cells showed a typical pattern of cell cycle with ~20% of cells in the G_2-M phase. Irrespectively of Brca1 status, a significant increase in G_2-M fraction of the cell cycle was observed at 24 and 48 h after treatment. The G_2-M fraction at 24 h increased in comparison with control cells in both treated BRCA1-wt and BRCA1-null cell lines. Additionally, an increasing population of polyploid cells was observed in treated MBA-MD-436 and UACC 3199 cells. It seems that the 17-AAG-treated BRCA1-null cells adapted to Hsp90 inhibition and reentered the cell cycle. Hs578T cell type has a mixed diploid and polyploid cell population. 17-AAG-induced growth inhibition was associated with cell cycle arrest in G_2-M phase reported in polyploid cells. Notably, the sub-G_0 fraction has doubled compared with the control in most of the cell lines after 48 h of treatment. No symptoms of cell senescence were observed in the cells halted at G_2-M, as they were negative to lysosomal SA-β-galactosidase staining at low pH (data not shown).

G_2-M Checkpoint Proteins Affected after Hsp90 Inhibition

It was expected that the 17-AAG treatment would degrade Hsp90 client proteins. Because a stop in G_2-M was observed in the breast cancer cell lines, we studied by Western blot known Hsp90 client proteins and other important regulators of the G_2-M checkpoint and compared them between the BRCA1-null and BRCA1-wt cell lines. In accordance to former studies (20), an increase in expression of Hsp90 and the cochaperone Hsp70 was observed in all

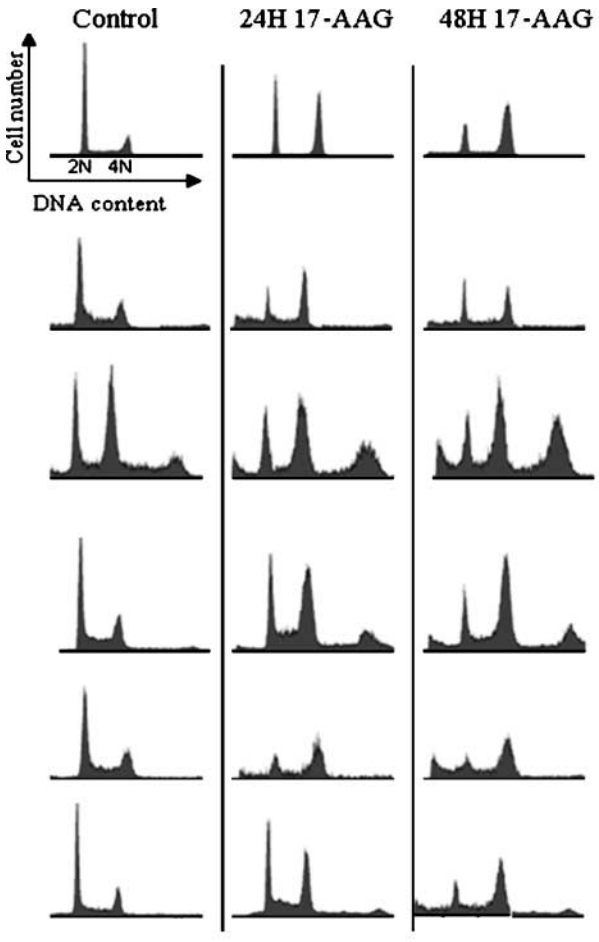

	Sub G0	G0/G1	G2/M (4 N)	8N
Control	1.31	52	20.91	
17-AAG 24H	1.26	37	57.85	
17-AAG 48H	8.02	21.89	61.23	
Control	9.49	46	21.59	
17-AAG 24H	24.36	16	38.81	
17-AAG 48H	20.76	22	31.51	
Control	4.99	21.43	39.9	11.45
17-AAG 24H	6.86	16.17	36.9	24.77
17-AAG 48H	11.23	13.18	29.9	31.73
Control	0.16	44.97	25.9	2.90
17-AAG 24H	1.56	21.64	41.4	12.8
17-AAG 48H	8.15	13.93	44.8	13.52
Control	5.53	44.13	24.74	
17-AAG 24H	14.70	18.55	46.52	
17-AAG 48H	28.54	11.12	39.97	
Control	3.51	49.31	20.99	-
17-AAG 24H	4.86	31.19	38.06	3.94
17-AAG 48H	18.7	30.82	35.51	5.04

Figure 2. 17-AAG arrests cells in G_2-M phase. DNA content was assessed with PI staining in control and treated cells with 500 nmol/L 17-AAG at 24 and 48 h. Typical histograms showing cell cycle distributions along with percentage of cells in each cell phase are represented.

cell lines after 17-AAG treatment. As consequence, several client proteins were degraded (Fig. 3). Chek1 is a well-documented Hsp90 client protein and regulates mitosis progression (21). A consistent depletion with time in BRCA1-wt cell lines was notified. Interestingly, a more significant reduction of the level of Chek1 was observed in all three BRCA1-null cell lines studied (Fig. 3). However, Chek2, another regulator of the G_2-M transition, was not affected by the 17-AAG treatment. It was shown previously that Chek1 but not Chek2 activation requires the function of Brca1 (17, 22), which may explain the differences in level of destabilization of the protein on treatment between BRCA1-null and BRCA1-wt cell lines. For G_2-M transition, the crucial complex is Cdc2/cyclin B. Cdc2 is a major mitotic kinase promoting chromosome condensation and nuclear breakdown for G_2-M transition. Although Cdc2 has not been described as a Hsp90 client, a significant decrease of total Cdc2 was observed only in BRCA1-null cell lines after 17-AAG but was not affected in BRCA1-wt cell lines, suggesting a regulation of Cdc2 by Brca1. After treatment, the inhibitory phosphorylation at Tyr^{15} of Cdc2 was, however, greater in cells that express Brca1. Cyclin B1 is a necessary cofactor of kinase activity. We found in all cell lines that cyclin B1 accumulated on treatment. In addition, Cdc25C, the phosphatase that dephosphorylates Cdc2, was also found increased on 17-AAG probably due to the degradation of Chek1. All these changes in the proteins that regulate G_2-M may explain that the cells finally are arrested before metaphase/anaphase transition.

Other already described Hsp90 client proteins involved in mitosis, such as survivin, Plk1, and Aurora B (23, 24), did not show any effect in their expression on treatment.

Brca1 Deficiency Induces Bypass of the G_2-M Checkpoint and Premature Mitosis after 17-AAG Treatment

We hypothesized that, on treatment with the drug, the majority of cell lines at first arrest in G_2 stage, with a

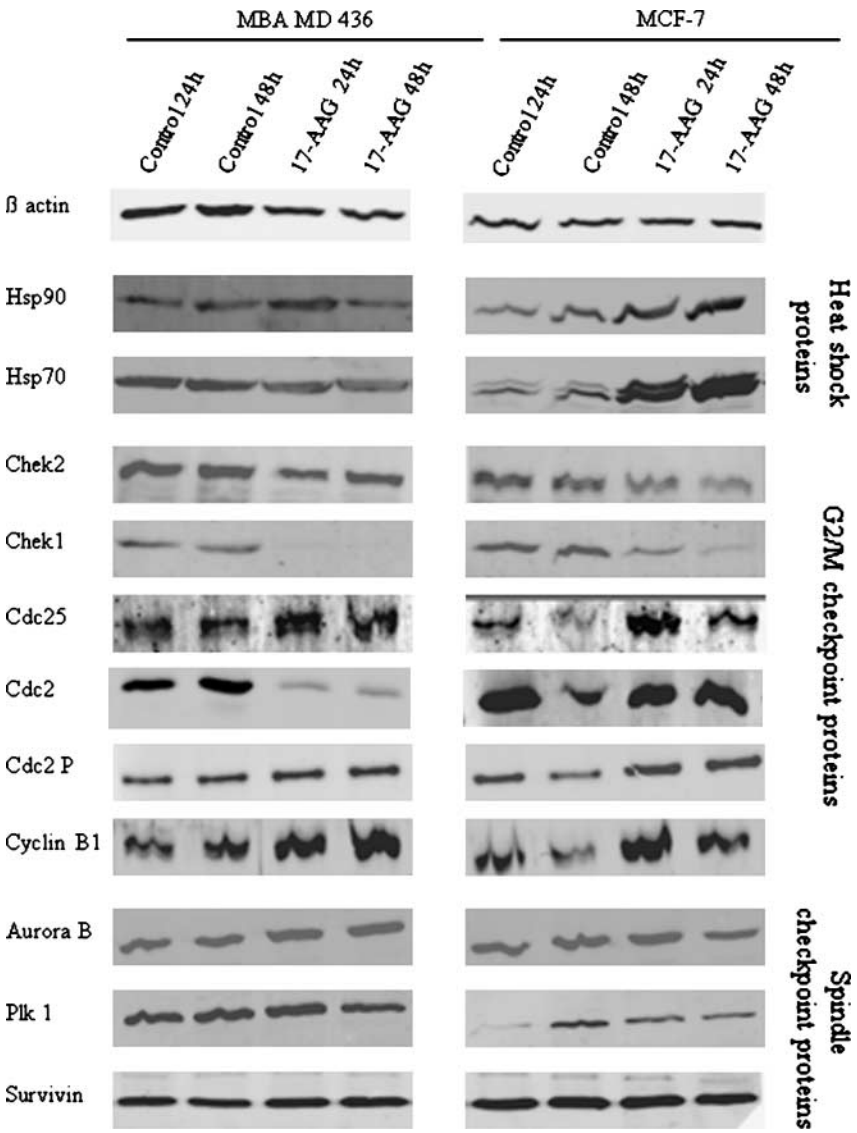

Figure 3. 17-AAG effects on cell cycle regulatory proteins in MCF-7 and MBA-MD-436 cell lines. Levels of Chek1, Chek2, Cdk2, Cdk2 phospho-Tyr^{15}, cyclin B1, Plk1, Aurora B, survivin, Akt, Hsp70, and Hsp90 were estimated in representative BRCA1-wt and BRCA1-null breast cancer cell lines by Western blot. β-Actin was used as a loading control.

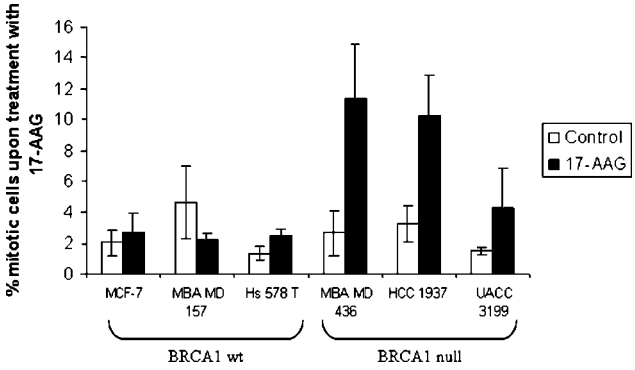

Figure 4. Significant increase in mitotic entry on treatment with 17-AAG in Brca1 mutated cell lines. Mean ± SD of three independent experiments. Mitotic index in control untreated cells (*white*) and cells after 48 h of incubation with Hsp90 inhibitor (*black*) is represented.

differential percentage of cells that overcome G_2-M transition checkpoint and enter aberrant mitosis, leading to mitotic catastrophe cell death. If Brca1 is involved in the checkpoint control, Brca1-deficient cells will present a higher number of cells in M phase after 17-AAG treatment. Expression of phospho-H3 varied from 1% to 3% in control cells of both BRCA1-wt and BRCA1-null cell lines. After treatment, all cell lines, except of MBA-MD-157, responded with an increase of phospho-H3 (Fig. 4). MCF-7 and Hs578T showed 2.6% and 2.5% of cells in mitosis, respectively, after treatment with 17-AAG. Surprisingly, premature mitotic entry in BRCA1-null cells after treatment increased drastically to 11.4%, 10.3%, and 4.2% in MBA 436, HCC 1937, and UACC 3199, respectively. Then, statistically significant differences in the entrance in mitosis were found between BRCA1-null and BRCA1-wt cells ($P = 0.04$). The data suggested that 17-AAG activates G_2-M checkpoint in BRCA-wt cells, delaying the movement of G_2 cells into mitosis phase. In contrast, 17-AAG treatment of BRCA1 mutant cells did not activate G_2-M checkpoint after 17-AAG treatment as those cells largely progressed into mitosis. Alternatively, it also could be that 17-AAG activates a mitotic specific blockage such as spindle checkpoint or chromosome separation.

Mitotic Catastrophe Cell Death in 17-AAG-Treated Cells

Typically, 17-AAG-treated cells show aberrant segregation of chromosomes, microtubule misalignment, multicentrosomes, or multipolar mitoses. Mitotic perturbances are correlated with mitotic entry frequencies. Predominantly BRCA1-null cell lines exhibited highest number of mitotic aberrations (Fig. 5). Clearly, cells with dysfunctional G_2-M checkpoint (MBA-MD-436, HCC 1937, and UACC 3199) enter more frequently into mitosis on 17-AAG treatment. Multiple centrosomes are characteristic feature of MBA-MD-436 cell line. Chromosome misalignments along the spindle and micronucleated cells were typically encountered in HCC 1937. Because low mitotic entrance was reported for BRCA1-wt cell lines, only few aberrant mitotic figures were present, with a predominance of

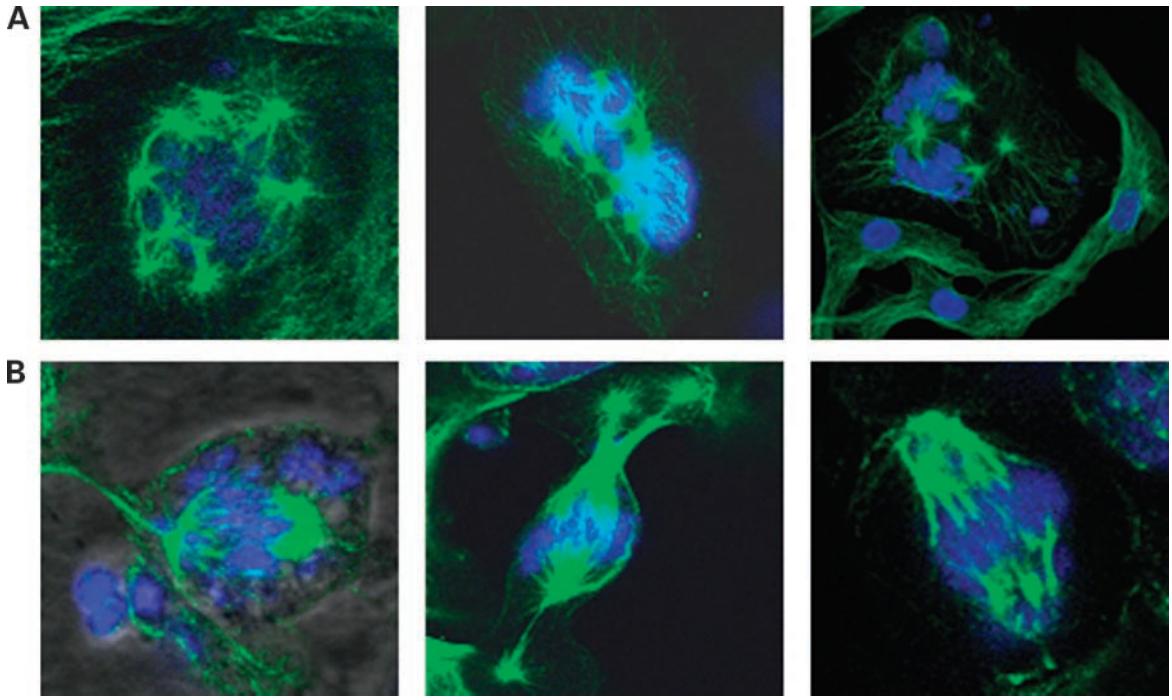

Figure 5. Mitotic catastrophe cell death on 17-AAG treatment. Forty-eight hours after treatment with 500 nmol/L 17-AAG, cells were collected and immunoassayed with anti-α-tubulin antibody counterstained with 4,6′-diaminidino-2-phenylindole. **A,** mitotic catastrophe figures showing multiple centrosomes, predominant in MBA-MD-436 cell line. **B,** metaphase spreads showing missegregation of chromosomes in HCC 1937 cell line and UACC 3199 cell line.

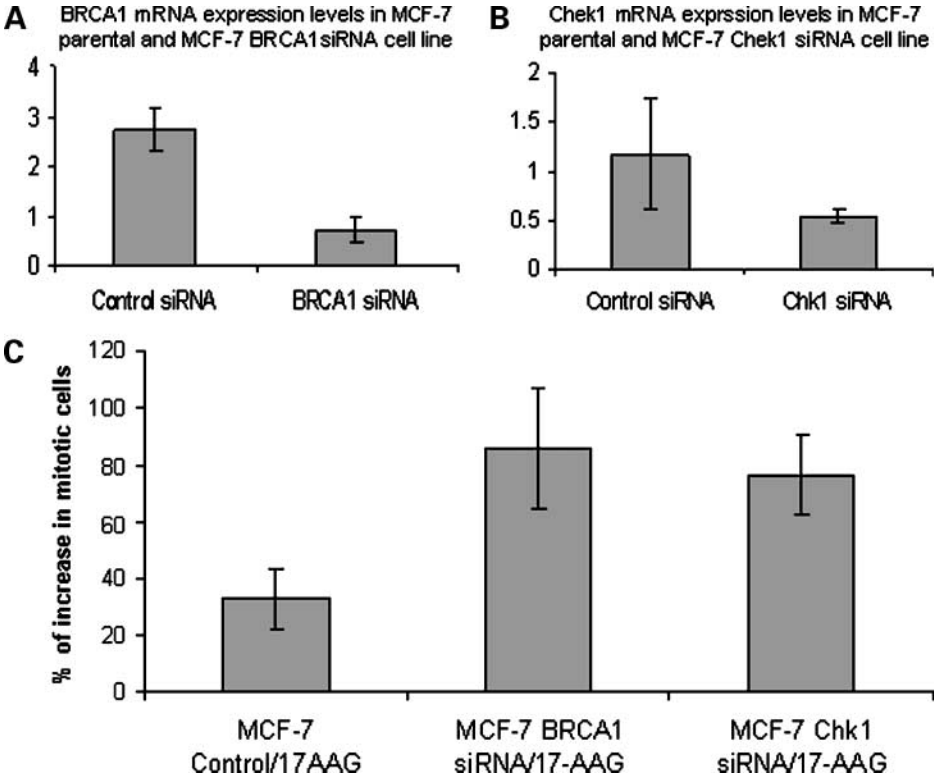

Figure 6. Brca1-mediated increase in mitotic entrance after 17-AAG. mRNA expression levels in MCF-7 treated with siRNA control and Brca1 siRNA (**A**) or Chek1 siRNA (**B**). siRNA-treated cells 24 h after silencing were incubated 36 h with Hsp90 inhibitor and harvested, and percentages of phospho-histone H3–positive mitotic cells were determined by fluorescence-activated cell sorting analysis by using double staining with PI and anti-phospho-histone H3. Increment in percentage of cells entering into mitosis is shown in Brca1-silenced cells and Chek1-silenced cells in MCF-7 cell line compared with wild-type MCF-7 on treatment with 17-AAG (**C**). *Bars,* SD.

apoptotic bodies (MBA-MD-157), and cells at prometaphase stage (MCF-7 and Hs578T). Dynamics of *in vivo* division are accessible in Supplementary Movie S1.[6] These data confirm that mitotic catastrophe was the primary mediator of cell death induced by 17-AAG.

Mitotic Catastrophe Cell Death Is followed by Apoptotic DNA Fragmentation

According to the cell cycle profile, a sub-G_0 increase was detected in all of the cell lines on treatment at 24 and 48 h. It is noteworthy that the sub-G_0 population increment followed decrease in G_2-M block. To further study cells in sub-G_0, the earliest apoptotic marker, Annexin V, was studied. An increment in early apoptosis was found (Annexin V–positive/PI-negative cells) followed by necrosis (Annexin V–positive/PI-positive) in all of the cell lines (Supplementary Fig. S1).[6] Exposure to 500 nmol/L 17-AAG after 48 h of treatment resulted in 5-fold increment in MCF-7 and 2- to 3-fold increments in apoptosis in MBA-MD-157, Hs578T, MBA-MD-436, HCC 1937, and UACC 3199 cell lines. Similar results were obtained for caspase-3 assay (data not shown). Our data indicate that, after 48 h of treatment, the BRCA1-null cell lines were undergoing predominantly mitotic catastrophe followed by apoptosis, whereas BRCA1-wt cell lines had a preponderance toward apoptotic like death and necrosis.

Brca1 Is Required for Active G_2-M after 17-AAG Treatment

Because the 17-AAG effect on mitotic index and on cell cycle regulatory proteins showed differences between BRCA1-wt and BRCA1-null cell lines, we have silenced the Brca1 expression in MCF-7 cell line to study the role of Brca1 in the differential response. MCF-7 transfected with control or Brca1 siRNA were exposed to the 500 nmol/L Hsp90 inhibitor. Transient silencing of Brca1 in MCF-7 cell line reduced Brca1 mRNA levels to 50% at 24 h ($P = 0.002$; Fig. 6A). Cells that lacked Brca1 showed 2-fold gains in mitotic index values compared with MCF-7 control cell line on treatment (Fig. 6C). It means that Brca1-deficient cell lines are more prone to bypass the G_2-M checkpoint and accumulate at metaphase, whereas Brca1-proficient cell types would be more stringently G_2-M arrested when subjected to 17-AAG.

Chek1 Deficiency in Brca1-Positive Cells Abrogates G_2-M Checkpoint

To determine whether Brca1-mediated activation of chek1 is responsible for G_2-M block by 17-AAG, we analyzed the effect of chek1 silencing on Brca1-positive cells. Over 50% depletion of chek1 ($P = 0.02$) in MCF-7 cell line was observed (Fig. 6B). Down-regulation of chek1 and subsequent 17-AAG treatment reduced the G_2-M checkpoint control in cells expressing Brca1 ($P = 0.009$) and sustained a more effective mitotic entrance as shown by mitotic marker phospho-H3 staining (Fig. 6C).

Discussion

In our study, we have examined the response of a panel of both BRCA1-wt and BRCA1-null breast cancer cell lines to Hsp90 inhibitor, 17-AAG. Our data indicate cytotoxic and cytostatic effect of the drug. Although we have notified that all the breast cancer cell lines analyzed exhibited similar

IC_{50}, we could identify differential form of death between BRCA1-null and BRCA1-wt cells followed by the treatment. We found that Hsp90 inhibitor induced G_2-M arrest in both BRCA1-wt and BRCA1-null cell lines analyzed; however, interestingly predominantly BRCA1-null cell lines displayed a significant mitotic index increase and cellular and nuclear morphology typical for mitotic catastrophe cell death. Mitotic arrested cells displayed chromosomes missegregation, microtubule misalignment, and multiple centrosomes. Furthermore, as a DNA repair process is impaired in Brca1-deficient cells, more aberrant mitotic figures were reported in HCC 1937, UACC 3199, and MBA-MD-436 cell lines after inhibiting Hsp90. The mitotic catastrophe cell death was followed by secondary apoptosis. On the contrary, MCF-7 and Hs578T cells showed a low increase in mitotic entrance, and MBA-MD-157 arrested in G_2-M phase of the cycle. The cells died mostly through apoptosis.

17-AAG strongly inhibited the cell growth of the breast cancer cell lines and affected the G_2-M regulatory proteins. We have found decreased levels of well-reported Hsp90 client protein, chek1, in hereditary cell lines. Interestingly, BRCA1-wt cell lines showed moderate decrease in the expression of chek1 after treatment, with up-regulated levels of Cdc2 phospho-Tyr^{15}, suggesting a much stronger halt at G_2-M phase compared with Brca1-deficient cells. Cyclin B1 levels were consistently high along breast cancer cell lines. Up-regulation of cyclin B1 and prolonged activation of cyclin B1/Cdc2 complex are typical features of mitotic catastrophe (25). It has been described previously that other cell cycle regulators such as Aurora B, survivin, and Plk1 are client proteins of Hsp90 (23, 24). According to our data neither Aurora B, survivin, nor Plk1 were affected after 17-AAG. This discrepancy occurs as those proteins may function as Hsp90 clients only in specific cell types. Moreover, we cannot discard that mutations in these proteins may affect Hsp90 binding.

Taking all into account, we showed that Brca1 contributes to the control of G_2-M following the 17-AAG treatment. There are also several studies in which Brca1 was reported to be engaged in several cell cycle checkpoints (16–18). In parallel, it is possible that other dissimilarities among the cell lines may be responsible for the differential effect, for example, in the mitotic index, cell cycle, or protein destabilization levels.

The siRNA experiments were done to directly study the role of Brca1 in the control of G_2-M after treatment with 17-AAG. By using Brca1-deficient or Brca1-proficient cells, we showed that Brca1-silenced cells were more prone to bypass the G_2-M checkpoint and accumulate at mitosis, whereas Brca1-proficient cell types would be more stringently G_2-M arrested when subjected to 17-AAG. Observation confirmed with previous studies using other drugs such as paclitaxel, vinorelbine, bleomycin (26), and genistein (27) and more recently by Yamane et al. (19) that has suggested that Brca1 may influence G_2-M checkpoint response to 6-thioguanine.

Loss of chek1 also resulted in weaker G_2-M checkpoint control. Essential activation of chek1 by Brca1 might explain why chek1 was almost completely depleted by Hsp90 inhibition in BRCA1-null breast cancer cell lines. Further, we proved that chek1-silenced cells highly entered mitosis in a BRCA1-wt cell line after treatment with 17-AAG. Interestingly, as reported (17), Brca1-proficient cells under treatment with chek1 inhibitor, UCN01, did not show G_2-M arrest after ionizing radiation. These data are in line with our results. Together, these results suggest that Brca1 mediates G_2-M arrest through chek1 activation. Moreover, Brca1 acts upstream chek1, regulating its expression, a data in accordance with previous work (17).

Taken together, we showed a connection between Brca1-dependent chek1 down-regulation and mitotic abnormalities induced by 17-AAG. To our knowledge, 17-AAG effects on breast cancer cell lines being Brca1 dependent yet were not suggested. However, we do not exclude that there might be other way, not mediated by chek1, by which Brca1 enhances G_2-M arrest in response to 17-AAG.

Mitotic catastrophe was a result of abrogated checkpoint after 17-AAG treatment. In the BRCA1-null cell lines, we have observed significant mitotic arrest, elevated levels of cyclin B1, and multiple defects in mitosis (chromosome disorganization, multiple centrosomes, multinucleated cells, and micronucleus), suggesting mitotic catastrophe as the predominant cell death. On the contrary, in BRCA1-wt cells, we have observed predominant apoptosis cell death followed by the 17-AAG treatment.

Considering the clinical application of Hsp90 inhibitors, the high affinity of 17-AAG to cancer cells is of high importance. Using immunohistochemistry and Western blot analysis, we and others (28) showed a higher protein level of Hsp90 in tumoral cells compared with normal tissues, which correlates with higher sensitivity to the drug. Finally, because clinical trials on 17-AAG are currently on and chemical genetics is in search of synthetic Hsp90 inhibitors, it may prove helpful to know that the drug effect might be differential in BRCA1-wt and BRCA1-null patients.

Disclosure of Potential Conflicts of Interest

No potential conflicts of interest were disclosed.

Acknowledgments

We thank the Group of Confocal Microscopy and Cytometry Unit from Centro Nacional de Investigaciones Oncológicas for help and advice and Maria Victoria Fernandez for the technical assistance.

References

1. Kamal A, Thao L, Sensintaffar J, et al. A high-affinity conformation of Hsp90 confers tumour selectivity on Hsp90 inhibitors. Nature 2003;425:407–10.

2. Mitsiades CS, Mitsiades NS, McMullan CJ, et al. Antimyeloma activity of heat shock protein-90 inhibition. Blood 2006;107:1092–100.

3. Senju M, Sueoka N, Sato A, et al. Hsp90 inhibitors cause G_2/M arrest associated with the reduction of Cdc25C and Cdc2 in lung cancer cell lines. J Cancer Res Clin Oncol 2006;132:150–8.

4. Schwock J, Pham NA, Cao MP, Hedley DW. Efficacy of Hsp90 inhibition for induction of apoptosis and inhibition of growth in

cervical carcinoma cells *in vitro* and *in vivo*. Cancer Chemother Pharmacol 2008;61:669 – 81.

5. Williams CR, Tabios R, Linehan WM, Neckers L. Intratumor injection of the Hsp90 inhibitor 17AAG decreases tumor growth and induces apoptosis in a prostate cancer xenograft model. J Urol 2007;178:1528 – 32.

6. Maloney A, Workman P. HSP90 as a new therapeutic target for cancer therapy: the story unfolds. Expert Opin Biol Ther 2002;2:3 – 24.

7. Neckers L. Heat shock protein 90: the cancer chaperone. J Biosci 2007;32:517 – 30.

8. Srethapakdi M, Liu F, Tavorath R, Rosen N. Inhibition of Hsp90 function by ansamycins causes retinoblastoma gene product-dependent G_1 arrest. Cancer Res 2000;60:3940 – 6.

9. Munster PN, Srethapakdi M, Moasser MM, Rosen N. Inhibition of heat shock protein 90 function by ansamycins causes the morphological and functional differentiation of breast cancer cells. Cancer Res 2001;61: 2945 – 52.

10. Schumacher JA, Crockett DK, Elenitoba-Johnson KS, Lim MS. Proteome-wide changes induced by the Hsp90 inhibitor, geldanamycin in anaplastic large cell lymphoma cells. Proteomics 2007;7:2603 – 16.

11. Sato N, Mizumoto K, Nakamura M, et al. A possible role for centrosome overduplication in radiation-induced cell death. Oncogene 2000;19:5281 – 90.

12. Nomura M, Nomura N, Newcomb EW, Lukyanov Y, Tamasdan C, Zagzag D. Geldanamycin induces mitotic catastrophe and subsequent apoptosis in human glioma cells. J Cell Physiol 2004;201:374 – 84.

13. Vogel C, Hager C, Bastians H. Mechanisms of mitotic cell death induced by chemotherapy-mediated G_2 checkpoint abrogation. Cancer Res 2007;67:339 – 45.

14. Mansilla S, Priebe W, Portugal J. Mitotic catastrophe results in cell death by caspase-dependent and caspase-independent mechanisms. Cell Cycle 2006;5:53 – 60.

15. Castedo M, Perfettini JL, Roumier T, Andreau K, Medema R, Kroemer G. Cell death by mitotic catastrophe: a molecular definition. Oncogene 2004;23:2825 – 37.

16. Zhu W, Dutta A. An ATR- and BRCA1-mediated Fanconi anemia pathway is required for activating the G_2/M checkpoint and DNA damage repair upon rereplication. Mol Cell Biol 2006;26:4601 – 11.

17. Yarden RI, Pardo-Reoyo S, Sgagias M, Cowan KH, Brody LC. BRCA1 regulates the G_2/M checkpoint by activating Chk1 kinase upon DNA damage. Nat Genet 2002;30:285 – 9.

18. Bae I, Rih JK, Kim HJ, et al. BRCA1 regulates gene expression for orderly mitotic progression. Cell Cycle 2005;4:1641 – 66.

19. Yamane K, Schupp JE, Kinsella TJ. BRCA1 activates a G_2-M cell cycle checkpoint following 6-thioguanine-induced DNA mismatch damage. Cancer Res 2007;67:6286 – 92.

20. Westerheide SD, Morimoto RI. Heat shock response modulators as therapeutic tools for diseases of protein conformation. J Biol Chem 2005; 280:33097 – 100.

21. Huang X, Tran T, Zhang L, Hatcher R, Zhang P. DNA damage-induced mitotic catastrophe is mediated by the Chk1-dependent mitotic exit DNA damage checkpoint. Proc Natl Acad Sci U S A 2005;102: 1065 – 70.

22. Arlander SJ, Eapen AK, Vroman BT, McDonald RJ, Toft DO, Karnitz LM. Hsp90 inhibition depletes Chk1 and sensitizes tumor cells to replication stress. J Biol Chem 2003;278:52572 – 7.

23. Fortugno P, Beltrami E, Plescia J, et al. Regulation of survivin function by Hsp90. Proc Natl Acad Sci U S A 2003;100:13791 – 6.

24. Georgakis GV, Li Y, Rassidakis GZ, Martinez-Valdez H, Medeiros LJ, Younes A. Inhibition of heat shock protein 90 function by 17-allylamino-17-demethoxy-geldanamycin in Hodgkin's lymphoma cells down-regulates Akt kinase, dephosphorylates extracellular signal-regulated kinase, and induces cell cycle arrest and cell death. Clin Cancer Res 2006;12: 584 – 90.

25. Castedo M, Perfettini JL, Roumier T, Kroemer G. Cyclin-dependent kinase-1: linking apoptosis to cell cycle and mitotic catastrophe. Cell Death Differ 2002;9:1287 – 93.

26. Quinn JE, Kennedy RD, Mullan PB, et al. BRCA1 functions as a differential modulator of chemotherapy-induced apoptosis. Cancer Res 2003;63:6221 – 8.

27. Tominaga Y, Wang A, Wang RH, Wang X, Cao L, Deng CX. Genistein inhibits Brca1 mutant tumor growth through activation of DNA damage checkpoints, cell cycle arrest, and mitotic catastrophe. Cell Death Differ 2007;14:472 – 9.

28. Pick E, Kluger Y, Giltnane JM, et al. High HSP90 expression is associated with decreased survival in breast cancer. Cancer Res 2007;67: 2932 – 7.

29. Charafe-Jauffret E, Ginestier C, Monville F, et al. Gene expression profiling of breast cell lines identifies potential new basal markers. Oncogene 2006;25:2273 – 84.

30. Neve RM, Chin K, Fridlyand J, et al. A collection of breast cancer cell lines for the study of functionally distinct cancer subtypes. Cancer Cell 2006;10:515 – 27.

31. Elstrodt F, Hollestelle A, Nagel JH, et al. BRCA1 mutation analysis of 41 human breast cancer cell lines reveals three new deleterious mutants. Cancer Res 2006;66:41 – 5.

Molecular Cancer Therapeutics

Mitotic catastrophe cell death induced by heat shock protein 90 inhibitor in BRCA1-deficient breast cancer cell lines

Magdalena Zajac, Maria Victoria Moneo, Amancio Carnero, et al.

Mol Cancer Ther 2008;7:2358-2366.